AD 715 550

DETERMINATION OF ATMOSPHERIC TRANSMISSIVITY FROM LASER BACKSCATTER MEASUREMENTS

SPACE SCIENCES LABORATORY

DISCLAIMER NOTICE

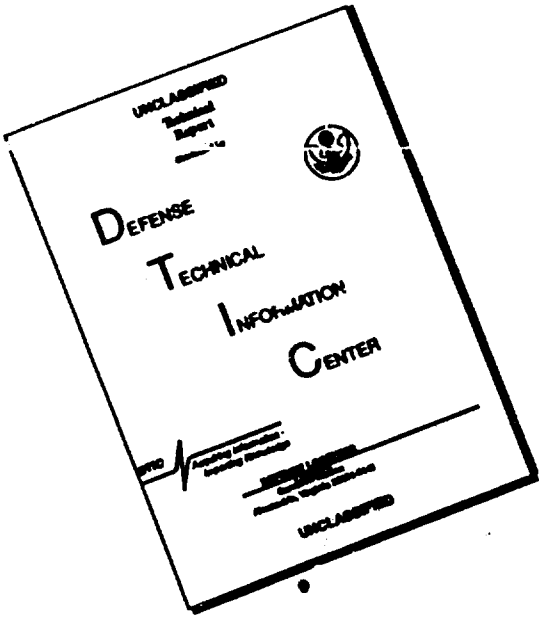

THIS DOCUMENT IS BEST QUALITY AVAILABLE. THE COPY FURNISHED TO DTIC CONTAINED A SIGNIFICANT NUMBER OF PAGES WHICH DO NOT REPRODUCE LEGIBLY.

SPACE SCIENCES LABORATORY

SPACE POWER AND PROPULSION RESEARCH

DETERMINATION OF ATMOSPHERIC TRANSMISSIVITY FROM LASER BACKSCATTER MEASUREMENTS

By

H. W. Halsey

E. L. Gray

MISSILE AND SPACE DIVISION

GENERAL ELECTRIC

CONTENTS

I. INTRODUCTION

A continuing program of atmospheric soundings with a laser radar has been in progress since early in March 1964*. The early stages of this program were devoted to gathering as much data as possible about as many different types of weather as possible[1]. As the program progressed it became apparent that significant advances in some areas of atmospheric measurement could be made. The most promising of these is the measurement of atmospheric transmission. The measurement of the transmission of the atmosphere at a given wavelength is difficult to obtain unless one has a convenient star very close to the direction in which the measurement is desired, then the measurement can be made only if the sensing equipment has been previously calibrated on this particular star. For applications in which the transmission must be measured rapidly over a wide arc of sky, there were, until recently, no methods available which would do this well. The measurement of atmospheric transmissivity has long been a problem for those making photometric measurements in the visible and infrared regions of the spectrum. Knowledge of the atmospheric transmissivity also finds application in the "slant visual range" problem which has plagued meteorologists associated with airports for many years. Several techniques have been developed over the years for making transmissivity measurements. These may all be assigned to one or the other of two basic groups of measurement devices. These two groupings are single ended and double telephotometers.

In this paper both groups are analyzed in the light of the Mie theory for the scattering of light by isotropic spherical particles. It is shown that

---

*-This program was supported in part by the U. S. Air Force as part of the TRAP program, partly by the Bell Telephone Laboratories as part of an infra-red data processing program and the remainder by the General Electric Company.

the double ended telephotometer has an inherent possibility of error when used to measure atmospheric transmissivity. The single ended telephotometer, on the other hand, offers the optimum technique for obtaining an error free measurement. The analysis of the single ended device is expanded and by deriving a relationship between the transmissivity, the intensity of light backscattered from the atmosphere and the elements of the scattering matrix, it is shown that the atmospheric transmissivity can be predicted by examining the backscattered light from a pulsed light source.

An experiment is performed in which a Q-switched ruby laser is used as the light source and atmospheric transmissivity is obtained by measuring the backscattered light. These measurements are compared with simultaneous transmissivity measurements taken on stars by conventional methods.

II. METHODS OF MEASUREMENT OF ATMOSPHERIC TRANSMISSIVITY

A. Star Measurements

The measurement of atmospheric transmissivity by stellar measurements has been a standard technique used by astronomers for many years. Some devices have been built whose sole function is the measurement of atmospheric transmissivity.

The basic technique requires a telescope equipped with a sensitive light detector, (generally a photomultiplier), a means of pointing the telescope and a cloudless night. The calibration of the equipment and subsequent use are next described. The telescope is pointed in the direction of the star but far enough away from it so that only light from the sky background enters the photodetector. The output of the photodetector is recorded. The telescope is moved directly on to the star and the photodetector output is again recorded. This process is continued while the star transverses the sky at least from horizon to zenith or from zenith to horizon as the case

may be. A graph is now plotted on which the ordinate values are the logarithmic photoelectric intensity of the star obtained by subtracting the sky background from the photoelectric intensity measured for both star and background. The abscissa values are a linear plot of number of effective atmospheres the starlight had to penetrate to reach the earth.

One effective atmosphere is defined as the amount of scattering atmosphere encountered when observing the star exactly at the zenith. For the flat earth case, two effective atmospheres result when the zenith angle is 60°, and so on. For the real case, corrections must be made for the curvature of the earth and atmospheric refraction, which is a function of both temperature and pressure. A graph of the effective atmospheres plotted as a function of elevation angle is shown in Figure 1. The data for the graph were plotted for a pressure of 760 mm of mercury and a temperature of 15° centigrade and taking the curvature of the earth into account. For all other pressures and temperatures a correction must be applied. The correction is made by multiplying the effective atmospheres by a quantity,

$$k = \frac{P}{760\,(0.962 + 0.0038t)}$$

where P is the actual pressure in millimeters of mercury and t is the actual temperature in degrees centigrade.

The graph is now made in which the actual photoelectric intensity of the star is plotted as a function of the number of effective atmospheres that the starlight passed through. A sample of such a plot, made for Jupiter on the night of October 18, 1964, is shown in the graph of Figure 2. A straight line is drawn through the array of points which represents the best fit possible. At small elevation angles, small errors in angle measurement can lead to large errors in the number of effective atmospheres. This is likely the explanation for the low data points near eight effective atmospheres. The straight line is extended to the zero atmosphere ordinate in order to obtain the limiting photoelectric intensity for the planet disk,

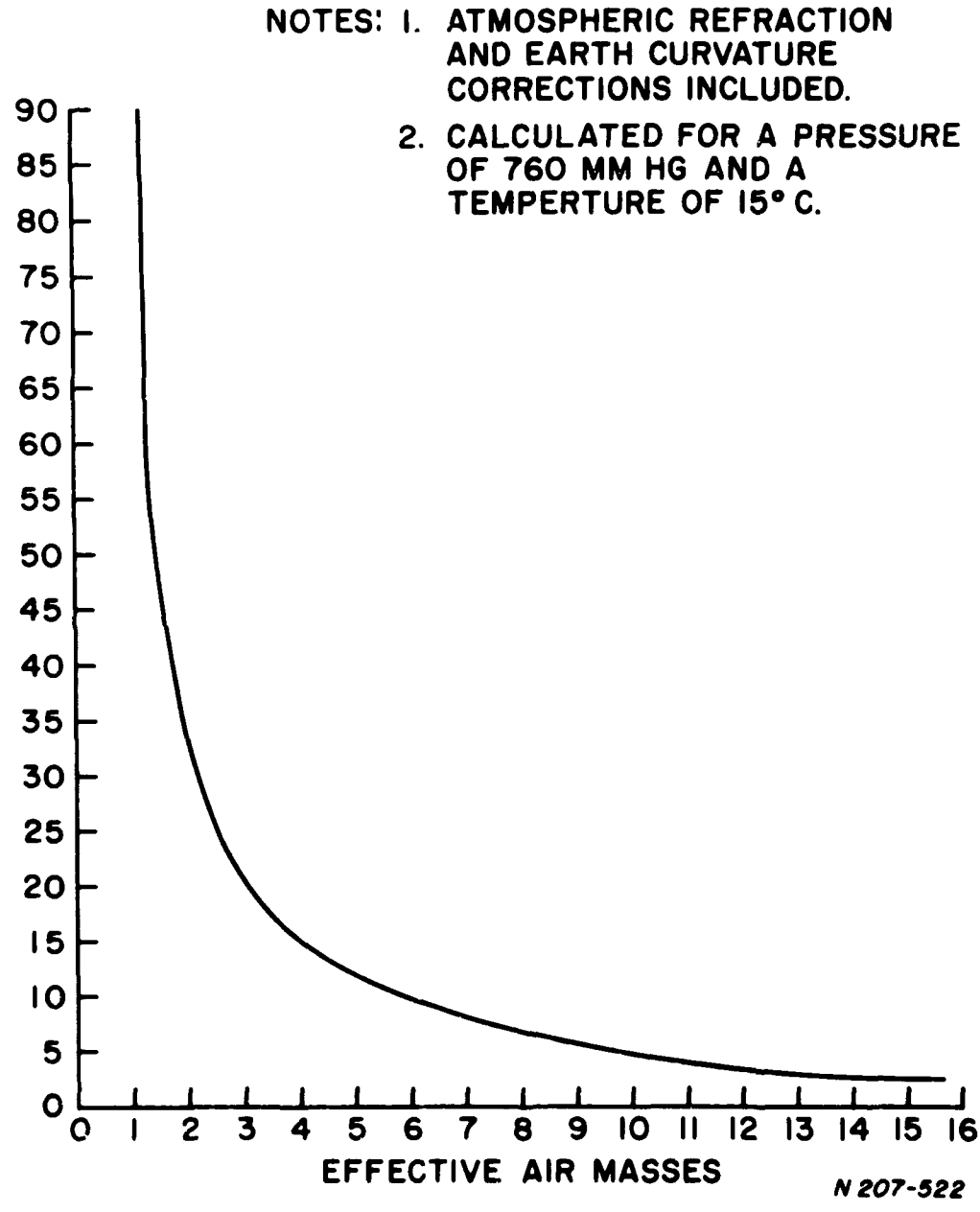

Figure 1. Effective Air Masses Plotted as a Function of Elevation Angle in Degrees.

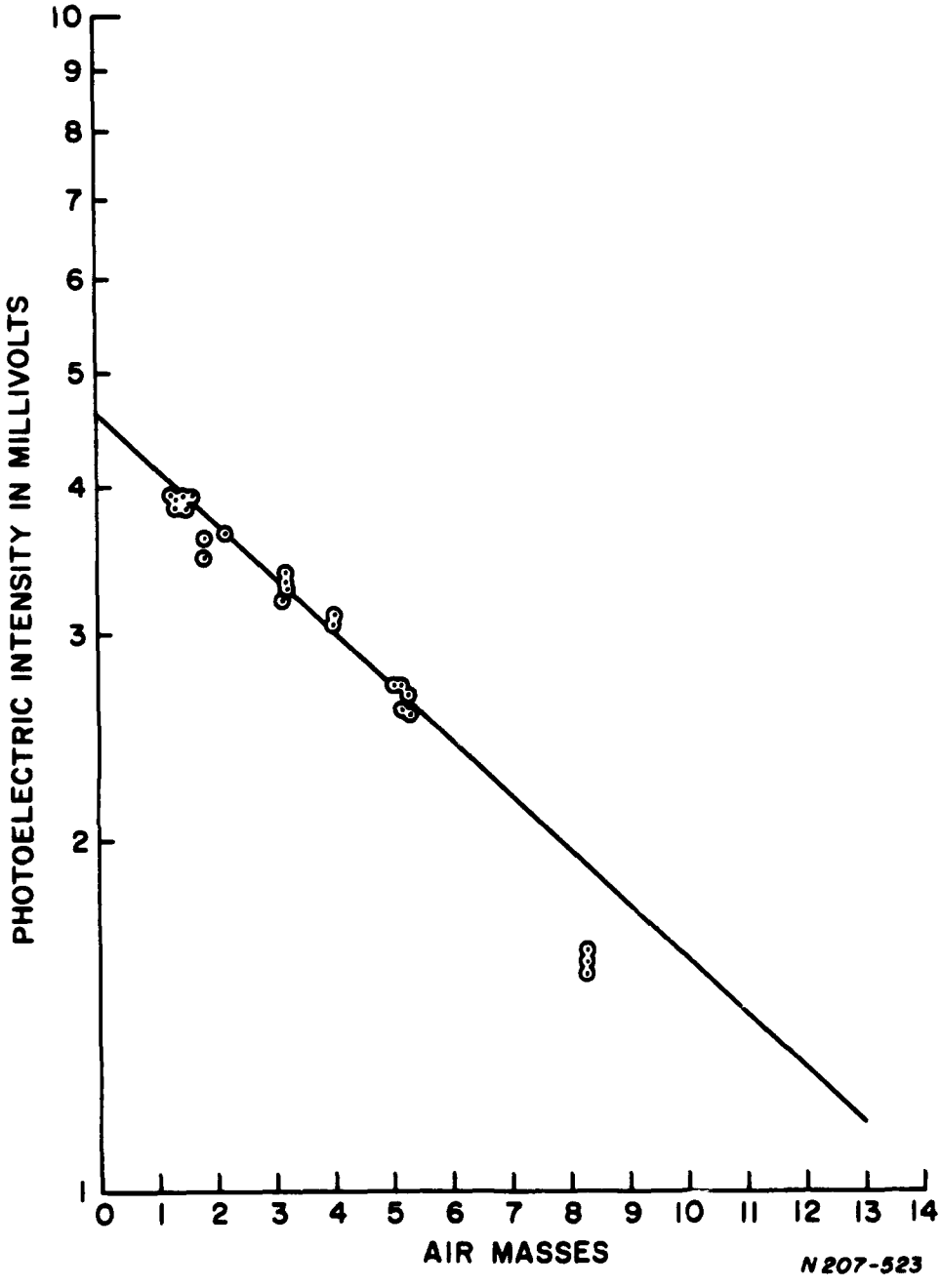

Figure 2. Photoelectric Intensity Plotted as a Function of Effective Air Masses for Jupiter on October 18, 1964.

or star as the case may be. The actual atmospheric transmission can now be obtained for any observation by dividing the limiting photoelectric intensity into the measured photoelectric intensity.

B. Telephotometers

The generic name "telephotometer" pertains to any instrument which measures light that comes from a distance. Telephotometers can be employed to measure atmospheric transmissivity in two general modes. In the first mode the telephotometer observes directly the light transmitted from a remote source. In the second mode the telephotometer observes only the scattered light from a source located at or near the telephotometer. In these applications it is convenient to refer to these instruments as double ended and single ended, respectively.

One fact should be made clear before the discussion is continued. That is that in spite of the large numbers of instruments available, none of them are in widespread use at meteorological stations (that is not surprising when one considers some of the instruments which have been developed).

These are, however, some techniques and instruments which do provide usable data as we shall see later in this discussion.

a. Double Ended Telephotometers

The use of double ended telephotometers is to be approached with caution. Several papers describing the errors associated with this application have been published[4, 5].

In addition more recent measurements [6] have borne out the conclusions reached in the earlier discussions. The basic discussion as given by Middleton[3] which considers this application is presented in partially paraphrased form below. The notation follows that of Middleton.

Assume that we have a telephotometer directed towards a distant light source with the encompassed atmosphere being illuminated only by the source. Light arrives at the telephotometer from all directions within a cone of half angle ψ about its axis. At a distance r_o, as diagrammed in Figure 3, let there be a source of intensity I_o in all directions within a cone of half-angle θ. Light from the source may reach the telephotometer in three ways:

(a) directly,

(b) after scattering in that portion of the atmosphere within the cone ψ,

(c) after two or more scatterings, a process which we shall neglect.

The extinction coefficient of the atmosphere is defined by Allard's law[7] which states that the illuminance produced by a distant light is

$$E = I r^{-2} e^{-\sigma r}$$

where I is the luminosity of the source, r is the range and σ is the extinction coefficient. The extinction coefficient, σ, thus accounts for the transmission losses due to scattering and absorption. Strictly speaking, σ is a function of the range along the direction of propagation considered, however there may be particular paths or portions of paths over which σ may be considered to be a constant.

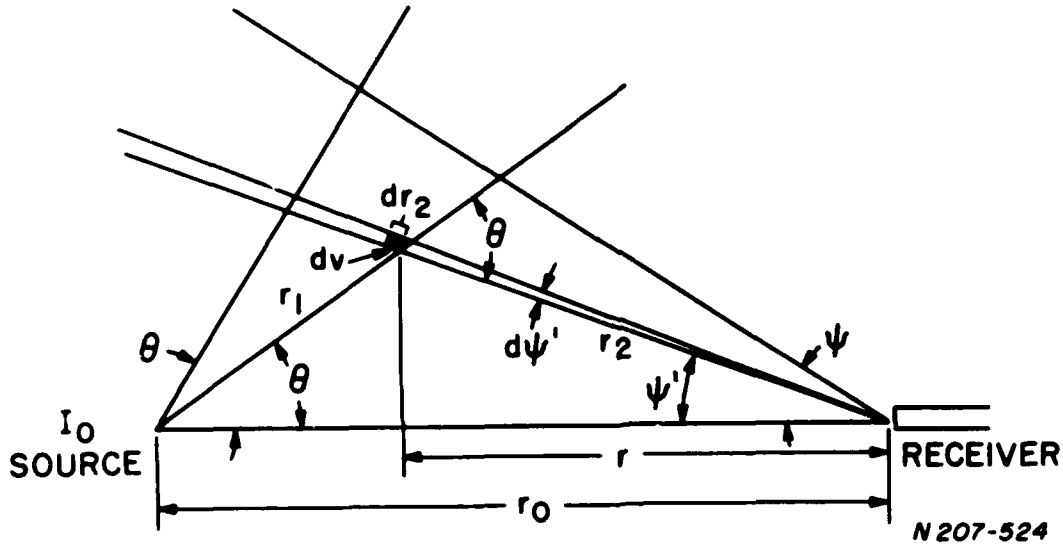

Figure 3. Illustrating the Double-Ended Telephotometer.

Under some conditions and for some purposes the losses due to absorption may be taken as negligible.

Now if we were to measure the extinction coefficient by observing a known source, we should measure only the direct light, knowing that the acceptance of the other components constitutes an error. This was mentioned in the references, and calculations were made on the restrictive assumption that both ψ and θ do not exceed one degree. This is perhaps adequate for ψ but neglects the important case of the telephotometry of a bare lamp, where $\theta = \pi$ radians. In this case we shall not restrict θ and put a limit of 3^{o} on ψ since no useful telephotometer will have an angular aperture greater than this. We shall further assume that:

(a) the atmosphere has everywhere an extinction coefficient σ,

(b) absorption may be neglected

(c) both the source and the entrance pupil of the telephotometer is small compared to r_o,

(d) there are no solid surfaces in a position to reflect light from the source to any part of the beam. In practice this means that the proximity of the ground is disregarded,

(e) the light is monochromatic of wavelength λ.

The direct light from the source produces an illuminance

$$E_a = I_o r_o^{-2} e^{-\sigma r_o} \qquad (2\text{-}1)$$

in the plane of the entrance pupil of the instrument.

The light scattered on may be calculated by considering a toroidal element of volume dv (Figure 3)

$$dv = 2\pi r_2^{2} \sin\psi' \, dr_2 \, d\psi' \qquad (2\text{-}2)$$

and calculating its intensity dI, in the direction of the telephotometer.

This is the product of the volume, the illuminance

$$E_1 = I_o r_1^{-2} e^{-\sigma r_1} \tag{2-3}$$

at dv and the scattering function $\beta'(\varphi)$. Writing $\sin\psi' = \psi'$, $\cos\psi' = 1$ (since $\psi \leq 3^o$), we find that

$$dI_1 = 2\pi r_2^2 I_o \frac{e^{-\sigma r_1}}{(r_o - r)^2 + r^2\psi^2} \beta'(\varphi)\, dr\, d\psi' \tag{2-4}$$

The illuminance at the telephotometer from this volume element is found by division by r_2^2 and multiplication by the transmittance of the air along the path r_2:

$$dE_2 = 2\pi I_o e^{-\sigma (r_1 + r_2)} \frac{\psi}{(r_o - r)^2 + r^2\psi^2} \beta'(\varphi)\, dr\, d\psi' \tag{2-5}$$

We now have to consider $\beta'(\varphi)$ and $e^{-\sigma (r_1 + r_2)}$. Since φ can assume any value it is unlikely that an analytic expression of any utility would approximate $\beta'(\varphi)$ for a foggy atmosphere and so we are obliged to produce a table of values. We find that for droplets of more than one or two microns diameter, there is a very large preponderance of forward scattering. This circumstance justifies neglecting light scattered by that portion of the atmosphere farther from the telephotometer than the lamp, and we may therefore write r_o for $(r_1 + r_2)$ in the expression $e^{-\sigma (r_1 + r_2)}$. We may now integrate equation (2-5) and obtain

$$E_2 = 2\pi I_o e^{-\sigma r_o} \int_o^{\psi} \int_o^{r_o} \frac{\psi\, \beta'(\varphi)\, dr\, d\psi'}{(r_o - r)^2 + r^2\psi^2} \tag{2-6}$$

for the illuminance scattered into the telephotometer, where φ may be expressed as a function of r and ψ' defined by

$$\sin\varphi = \frac{r_o\, \psi'}{[(r_o - r)^2 + r^2\psi'^2]^{1/2}}$$

This must of course be integrated numerically. The value of E_2 thus obtained represents the scattered light received by the photometer in addition to the directly received light. The fractional error in the measurement of E_a is simply the ratio E_2/E_a.

The graph of Figure 4 shows the results of such a calculation. The letters A, B, C, and D on the graph refer to the four sets of conditions set out in Table 1. Note that Table 1 indicated that conditions B and D differ by the size and number of the drops, but are otherwise similar.

Examination of Figure 4 will show that the percentage error in measured illuminance can be enormous. Case A represents a lamp at about the daylight visual range of ordinary objects. The error naturally decreases as the distance decreases, and almost proportionally. The most striking feature of the results is the much smaller error with larger droplets (compare case B and D). An actual fog will contain droplets of all sizes and it is obvious that there will be no universal relation between this error and the value of σ.

In the design of telephotometers then, it is obvious that the field of view ψ of the instrument should be kept small. Further data in the original papers show that the field illuminated by the lamp, θ, is of less importance, and makes little change after it gets to 0.1 radian.

These results have been confirmed by experiment[6] by utilizing a telephotometer with a variable field of view in periods of varying natural fog. The errors measured amounted to about five times that calculated for case A, probably because of the large numbers of smaller droplets present in the natural fog. We may conclude that a large and variable error is inherent in such measurements as may be made with a telephotometer of the double ended variety. In a permanent installation it might be possible to provide a series of screens at regular intervals along the optical path each with a hole slightly larger than the aperture of the telephotometer. This technique would aid in minimizing errors due to scattered light, but the

TABLE 1

Conditions Dealt with in Figure 4

Curve	Radius of Droplets in microns	Number per m^3	σ- (m^{-1})	Distance r_o (m)
A	2.5	10^8	3.93×10^{-3}	1000
B	2.5	10^8	3.93×10^{-3}	500
C	2.5	10^8	3.93×10^{-3}	200
D	10	6×10^6	3.93×10^{-3}	500

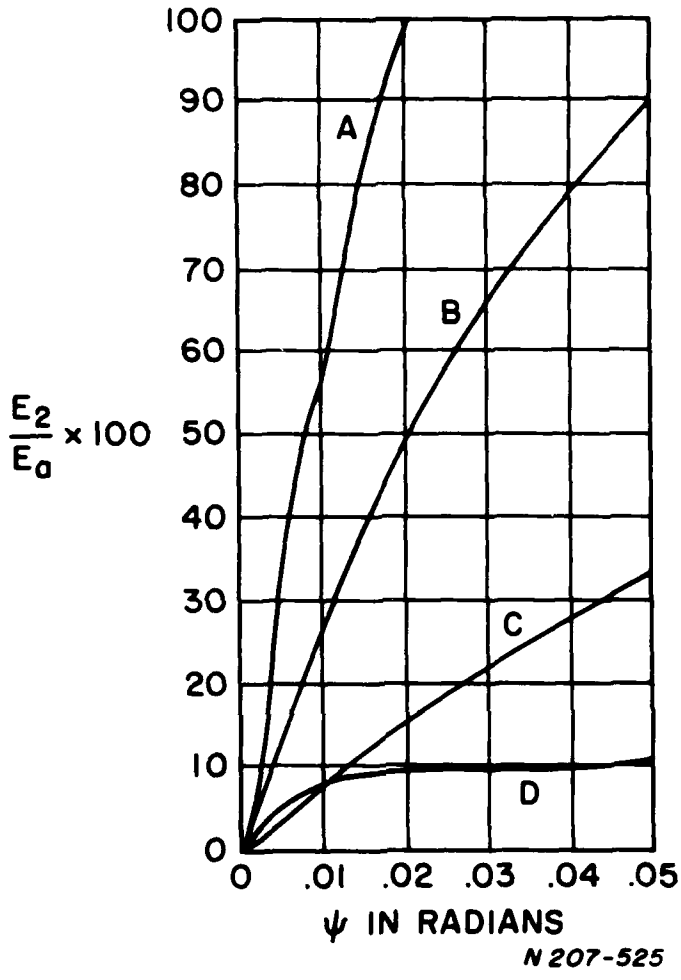

Figure 4. Calculations of percentage error of a measurement with a telephotometer having the half angle openings shown by the abscissa. (Mode for hypothetical atmosphere described in Table 1.).

installation, alignment and upkeep of such a system might not be worth the improvement in data quality obtained by its use. This technique is not applicable in the present context.

b. Single Ended Telephotometers

The single ended application of the telephotometer offers a very promising technique for the measurement of atmospheric transmissivity. Basically the single ended telephotometer depends upon the backscattered light to obtain its information about atmospheric transmissivity. If one neglects absorption as is possible in many practical situations, then scattering remains the sole contributor to the attenuation of light passing through the atmosphere (other than the inverse square geometric loss).

The single ended telephotometer is designed to obtain a measure of the scattering qualities of an atmosphere by observing light which is directly backscattered from the scattering media. From this data then, the forward scattering qualities of the media can be deduced and the atmospheric transmissivity readily obtained.

To illustrate the ideas of scattering theory, let us consider the scattering of a scalar plane wave[8]. The incident disturbance may be taken in complex form as

$$\mu_o = e^{-ikz + i\omega t} \tag{2-7}$$

which represents a sinusoidal wave of unity amplitude moving in the positive z direction.

After scattering, at distances from the particle large compared to the wavelength, the wave is an outgoing spherical wave

$$\mu = S(\theta, \varphi) \frac{e^{-ikr}}{ikr} \mu_{o_{z=0}} = S(\theta, \psi) \frac{e^{-ikr + i\omega t}}{ikr} \tag{2-8}$$

where the amplitude function $S(\theta, \varphi)$ is a function of the scattering angles

θ and φ only, and must be determined by a detailed analysis of the scattering problem. The above form is chosen so that $S(\theta, \varphi)$ is a pure (non dimensional number). The amplitude function may be complex indicating a phase shift. Using equation (2-7) the time dependence can be eliminated from (2-8) to obtain an additional form commonly used.

$$\mu = S(\theta, \varphi) \quad \frac{e^{ikz - ikr}}{ikr} \quad \mu_o \tag{2-9}$$

In the case of electromagnetic radiation, the incident disturbance and the scattered wave are transverse vector waves which can be characterized by giving the two components of the electric field perpendicular to the direction of propagation. These two components are specified in terms of their orientation with respect to the scattering plane (the scattering plane is defined as the plane formed by the two vectors describing the direction of propagation of the incoming wave and the particular outgoing ray considered. Using the suffixes l and r to characterize the components parallel and perpendicular to the scattering plane respectively, we note that since only linear processes are involved, the scattered components, E_l and E_r, are each linear combinations of the incident components, E_{lo} and E_{r_o}.

The relationship can be expressed in matrix form in close analogy with equation (2-9):

$$\begin{pmatrix} E_l \\ E_r \end{pmatrix} = \begin{pmatrix} S_2 & S_3 \\ S_4 & S_1 \end{pmatrix} \quad \frac{e^{ikz - ikr}}{ikr} \quad \begin{pmatrix} E_{lo} \\ E_{r_o} \end{pmatrix} \tag{2-10}$$

where again the quantities Si are functions of angle only. If we know the amplitude functions, we know everything (both amplitude and polarization) about the scattered wave.

In general, each component of the electric field is characterized by its amplitude and phase. Unfortunately, most optical measurements involve the light intensity. Therefore, it is desirable to define a set of parameters

which characterize a wave and relate the intensities and both the amplitude and phase of each component, and which also transform linearily from the incoming state to the outgoing state. Since we have two field components (E_l and E_r) and since we must know the amplitude and phase of each component, we must have four parameters to characterize the wave. These four parameters - which transform linearily from the incoming to the outgoing state - are called Stokes parameters. We shall now define them.

The electric field can be written as

$$\bar{E} = \mathrm{Re}\,(\hat{l}\,E_l + \hat{r}\,E_r) \tag{2-11}$$

where $\hat{l}$ and $\hat{r}$ are unit vectors in the parallel and perpendicular directions respectively, where Re indicates the real part.

Furthermore,

$$E_l = a_l e^{-i\epsilon_l - ikz + i\omega t}$$

$$E_r = a_r e^{-i\epsilon_2 - ikz + i\omega t} \tag{2-12}$$

where a_l and a_r are the amplitudes and ϵ_l and ϵ_2 are the phases. Clearly the amplitudes, a_l and a_r, can be expressed as

$$a_l^2 = E_l E_l^*$$

$$a_r^2 = E_r E_r^* \tag{2-13}$$

where the asterisk denotes the complex conjugate. To express the phases we see that the variables

$$U \equiv E_l E_r^* + E_r E_l^* = 2 a_l a_r \cos(\epsilon_l - \epsilon_2) \tag{2-14}$$

and

$$V \equiv i(E_l E_r^* - E_r E_l^*) = 2 a_l a_r \sin(\epsilon - \epsilon_2) \tag{2-15}$$

characterize the phase difference $\epsilon_1 - \epsilon_2$.

Thus the two quantities

$$I = E_l E_l^* + E_r E_r^* \tag{2-16}$$

$$Q = E_l E_l^* - E_r E_r^* \tag{2-17}$$

plus U and V as defined above enable us to determine the amplitudes and phases of E_l and E_r and we call these the Stokes parameters. Since E_l and E_r can be expressed as linear combinations of E_{lo} and E_{ro}, I, Q, U and V are quadratically dependent on E_{lo}, E_{ro} and their respective complex conjugates. Also, the quantities $E_{lo}E_{lo}^*$, $E_{lo}E_{ro}^*$, $E_{ro}E_{ro}^*$ and their complex conjugates can all be expressed as linear combinations of I_o, Q_o, U_o, and V_o. Therefore the Stokes parameters I, Q, U and V characterizing the scattered radiation can be expressed as linear combinations of I_o, Q_o, U_o and V_o. In Matrix form we can write this statement as:

$$\begin{pmatrix} I \\ Q \\ U \\ V \end{pmatrix} = \begin{pmatrix} L_{11} & L_{12} & L_{13} & L_{14} \\ L_{21} & L_{22} & L_{23} & L_{24} \\ L_{31} & L_{32} & L_{33} & L_{34} \\ L_{41} & L_{42} & L_{43} & L_{44} \end{pmatrix} \begin{pmatrix} I_o \\ Q_o \\ U_o \\ V_o \end{pmatrix} \tag{2-18}$$

The matrix L is called the scattering matrix. Clearly, if we know the components S_i of the amplitude function in equation (2-10), we can calculate the components L_{ij} in a straightforward manner.

All the previous considerations have been completely general. In a particular scattering problem we must solve Maxwell's equations with the appropriate boundary conditions and from this solution we may calculate the S_i and the L_{ij}. If the scattering particles are spheres, the above

program can be carried through and this particular case is called the Mie theory.

Without carrying out these calculations, which are quite lengthy, certain results of Mie's theory of scattering of light from spherical particles will be stated.

1. If the scatterers are spheres, the off-diagonal amplitude functions in equation (2-10) are zero.

   Therefore,

$$E_1 = S_2 \frac{e^{ikz - ikr}}{ikr} E_{1o} \tag{2-19}$$

and

$$E_r = S_1 \frac{e^{ikz - ekr}}{ikr} E_{ro} \tag{2-20}$$

So, if the incoming wave is polarized ($E_{1o} = 0$ or $E_{ro} = 0$), then the scattered wave will also be polarized.

2. Direct calculation shows that the components $L_{13} = L_{14} = 0$ in the scattering matrix. Therefore, the intensity I, (which is the sum of the squares of the amplitudes) depends only on I_o and Q_o, that is

$$I = L_{11} I_o + L_{12} Q_o \tag{2-21}$$

From equations (2-14) and (2-18) we see that if the incoming light is unpolarized, i.e., "natural light", then $A_1 = A_r$ and

$$Q_o = E_{1o} E_{1o}^* - E_{ro} E_{ro}^* = A_1^2 - A_r^2 = 0 \tag{2-22}$$

Therefore, if we wish to calculate the scattered intensity, I, of unpolarized incident light which has been scattered from a sphere, we need to know only L_{11} and the incident intensity. However, if the incident light is polarized, then it appears that we must know both L_{11} and L_{12} as well as I_o and Q_o in order to calculate I, equation (2-21).

Actual calculations of L_{11} and L_{12}[9], however, show that L_{12} is at least an order of magnitude smaller than L_{11}, and in the case of direct backscattering $L_{12} = 0$. Therefore, even with polarized incident light, if we wish to calculate the backscattered intensity, we need only L_{11}.

3. The results of the Mie theory also show that the L_{ij} depend on the radius of the scatterer. When considering the problem of atmospheric scattering, the size of the atmospheric aerosols varies widely. Therefore we must assume a density distribution of aerosols as a function of size and then integrate L_{11} over these sizes in order to find the net backscattered intensity. If ρ is the density distribution of aerosols as a function of radius, a, then

$$\bar{L}_{11} = \int_o^\infty \rho L_{11} \, da \tag{2-23}$$

$$I = \bar{L}_{11} I_o \tag{2-24}$$

If β is defined as the volume coefficient of scattering so that the intensity of light scattered from a volume dV is $\beta I_o \, dV$ (where I_o is the incident intensity on the volume dV), then we can define a normalized quantity,

$$\hat{\bar{L}}_{11} \equiv \frac{\bar{L}_{11}}{\beta} \tag{2-25}$$

The physical meaning of $\hat{\bar{L}}_{11}$ is as follows. The total intensity of light scattered by a volume dV into all directions is

$$I_{scat} = \beta I_o \, dV \tag{2-26}$$

This scattered radiation has an angular distribution $\delta(\theta, \omega)$, such that

$$\delta(\theta, \omega) \frac{d\Omega}{4\pi} \tag{2-27}$$

is the amount of I_{scat} which is scattered into a solid angle $d\Omega$. Therefore

$$(\beta I_o \, dV) \, \delta(\theta,\varphi) \, \frac{d\Omega}{4\pi} = \bar{L}_{11} \, I_o \, dV \, d\Omega \tag{2-28}$$

Hence

$$\delta(\theta,\varphi) = \frac{\bar{L}_{11} \, 4\pi}{\beta} = \hat{\bar{L}}_{11} \tag{2-29}$$

Thus $\hat{\bar{L}}_{11}$ describes the angular distribution of the light scattered from a volume, dV. It is this quantity, $\hat{\bar{L}}_{11}$, which has been calculated in detail[9], that is used to interpret the results of backscattered light experiments.

We now turn our attention to a more detailed analysis of a specific type of single ended telephotometer[10]. Let us consider a device which provides a short pulse of monochromatic light as the source, such as a Q-switched ruby laser. The geometry of the situation is shown in Figure 5. The source and the receiver are mounted coaxially at the origin. We make the stipulation that the receiver beam width is always greater than the transmitted beam width and that the beams have a half-angle width of less than 0.5°. The pulse of light goes out at some zenith angle ψ and at some range r the pulse illuminates a volume of aerosol defined by the pulse length L and the cross sectional area of the pulse A(r). The value of L is independent of r while the value of A(r) is of course a function of r. The altitude of the defined volume above the reference plane is Z.

The objectives of this analysis are twofold. First we wish to determine the backscatter from a laser pulse traversing an atmosphere of aerosol particles, and second to suggest a relationship between the transmissivity, T, of the atmosphere and the parameter X which is defined by

$$X \equiv \int_o^{\infty} r^2 \, \frac{E_s}{E_o} \, dr \tag{2-30}$$

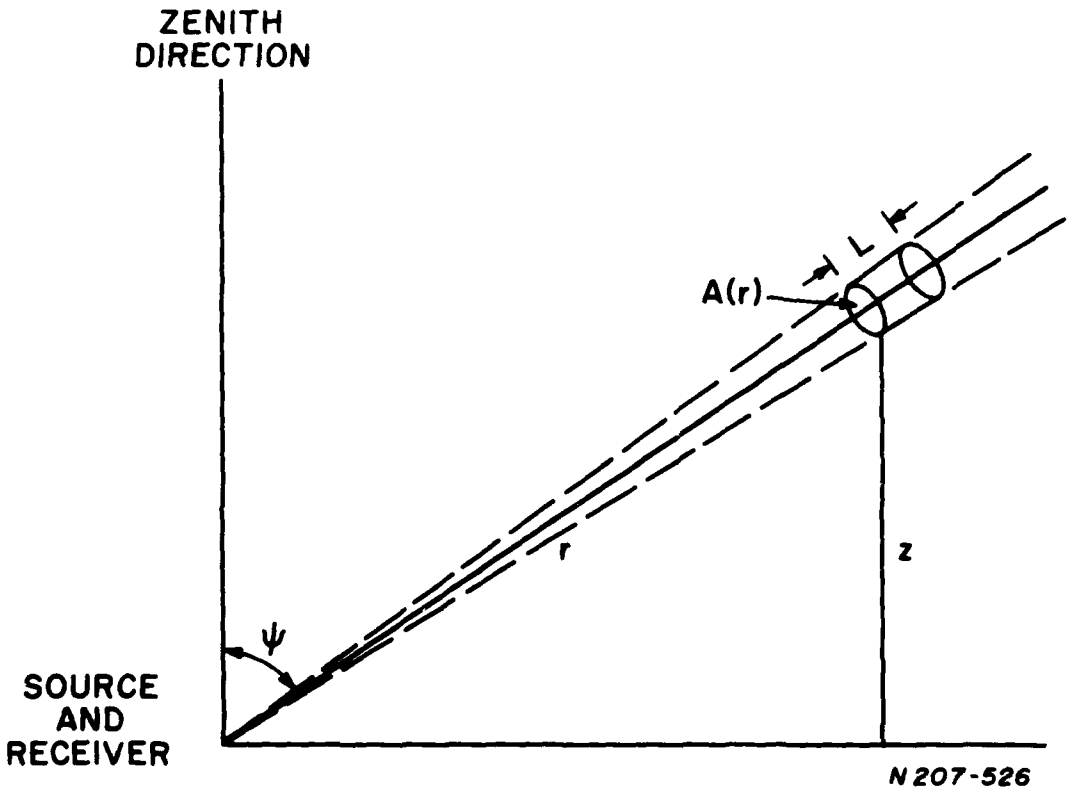

Figure 5. Geometry of Single Ended Telephotometer.

r = radial distance from the source

E_s = backscattered energy (per unit area normal to the direction of propagation)

E_o = source energy

It is convenient to discuss these objectives more or less simultaneously. With additions to the above notation, the following symbols will be employed.

E_t = energy transmitted to top of atmosphere

L = length of pulse

ψ = zenith angle

Z = altitude

$\beta(Z)$ = volume scattering coefficient

$\tau(Z) = \int_o^Z \beta(\xi)\, d\xi$ = normal optical depth

$\hat{\bar{L}}_{11}(180)$ = normalized matrix element in the Mie scattering theory such that $\bar{L}_{11}(180)/4\pi$ represents the fraction of the total amount of energy scattered from a unit volume of an aerosol into a unit solid angle in a direction measured at 180° to the direction of propagation (direct backscatter).

$A(r)$ = cross section area of light pulse at range r.

It has been calculated by Fraser[9] that the value for $\hat{\bar{L}}_{11}(180)$ is 0.259 at 0.625/micron. Implicit in this figure is a size distribution of aerosol particles in a unit volume. This distribution is reproduced in Figure 6, and represents a mean continental aerosol. According to Fraser this model has a volume scattering coefficient of $\beta = 1.06 \times 10^{-8}$ cm^{-1} at the surface. However, in order to incorporate experimentally measured values for β, the actual $\beta(Z)$ used was taken from a compilation by Elterman[11] for 0.7 micron. The agreement is close, Elterman's surface value being 1.35×10^{-8} cm^{-1}. We interpret Fraser's distribution then, as a relative one, and further assume that the size distribution is independent of altitude.

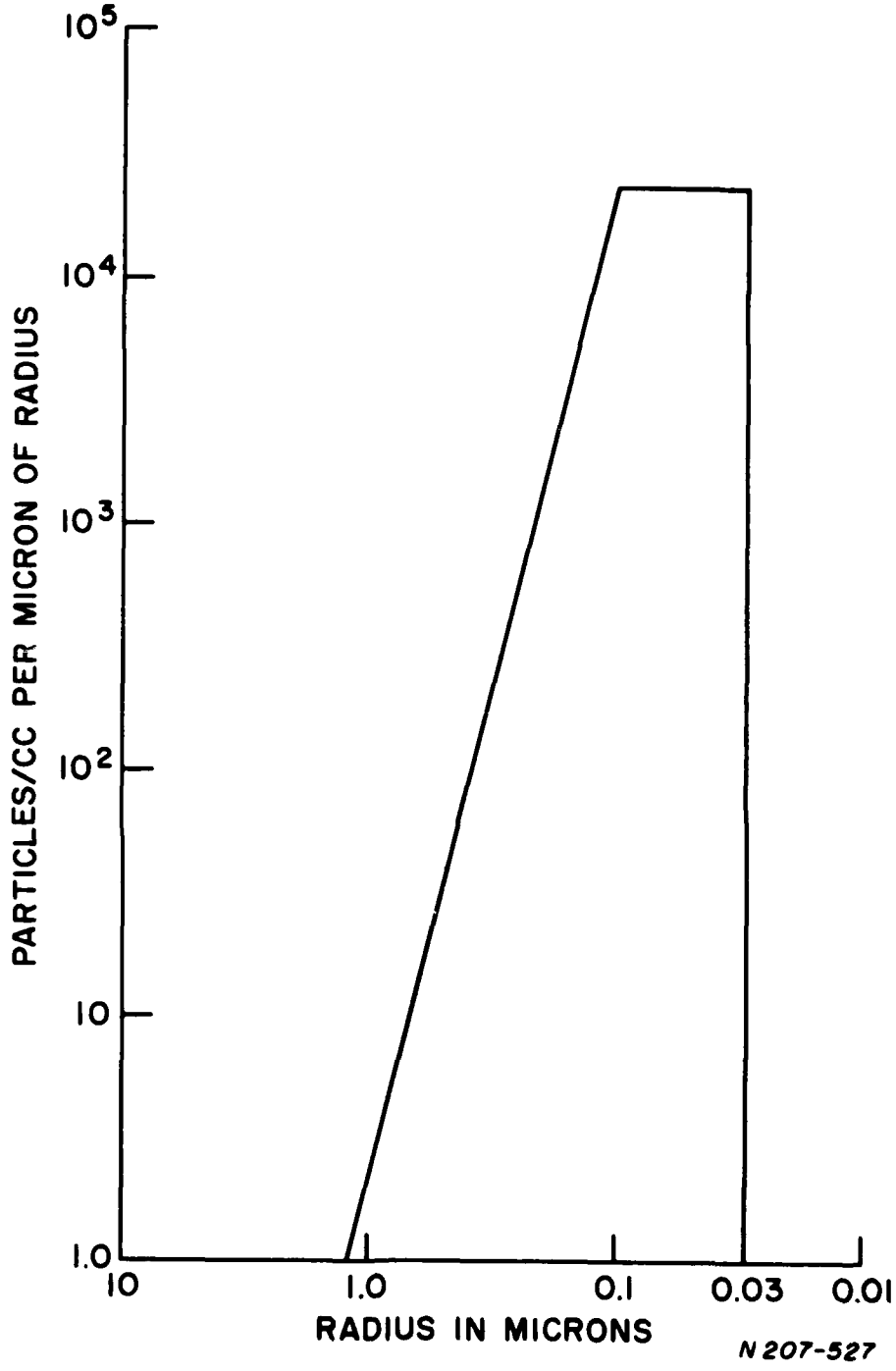

Figure 6. Size Distribution of a Mean Continental Aerosol. (Fraser).

Hence we take $\hat{\underline{L}}_{11}(180)$ as not depending on Z. It must be remembered however that $\hat{\underline{L}}_{11}$ is deperdent upon wavelength.

One further observation should be made before proceeding. That is, in calculating attenuation, the assumption is usually made that scattered light is lost from the beam in all directions. However, with a divergent beam, a portion of the forward scattered light may be retained, and the optical depth appropriately augmented. Computations showed, however, that for the extremely small solid angle under consideration, this possibility could be completely ignored.

With these preliminaries past, we consider the following:

In reference to Figure 5, let the pulse position be r or $Z = r \cos \psi$.

If E_o is the energy of the source, the energy arriving at the scattering volume is

$$E_o \; e^{-\frac{\tau(Z)}{\cos \psi}}$$

The energy per unit area at this volume is of course

$$\frac{E_o \; e^{-\frac{\tau(Z)}{\cos \psi}}}{A(r)}$$

The volume scatters an amount in all directions equal to

$$\beta(Z)\, dV \; \frac{E_o \; e^{-\frac{\tau(Z)}{\cos \psi}}}{A(r)} = \beta(Z)\, A(r)\, L \; \frac{E_o \; e^{-\frac{\tau(Z)}{\cos \psi}}}{A(r)} = \beta(Z)\, L\, E_o \; e^{-\frac{\tau(Z)}{\cos \psi}} \qquad (2\text{-}31)$$

Of this amount

$$\frac{\hat{\underline{L}}_{11}(180)}{4\pi}\, d\Omega\, \beta(Z)\, L\, E_o \; e^{-\frac{\tau(Z)}{\cos \psi}}$$

is scattered into the 180^o direction confined to a solid angle $d\Omega$. This solid angle $d\Omega$, would be that angle subtended by the detector. We will take, however, $d\Omega = \frac{1}{r^2}$ and the quantity E_s must be multiplied by the detector area in cm^2. Finally then, since the return trip suffers an additional

attenuation, we have

$$\frac{E_s}{E_o} = \frac{1}{r^2} \; e^{-\frac{2\tau(Z)}{\cos\psi}} \; L\beta(Z) \; \frac{\hat{\bar{L}}_{11}(180)}{4\pi} \tag{2-32}$$

This quantity is shown plotted in the graphs of Figure 7 and Figure 8. In Figure 8, the ratio is plotted as a function of altitude Z, whereas Figure 9 shows the radial distance (time) dependence.

As for the transmissivity we have:

$$E_t = E_o \; e^{-\frac{\tau(\infty)}{\cos\psi}} \tag{2-33}$$

then

$$T = \frac{E_t}{E_o} = e^{-\frac{\tau(\infty)}{\cos\psi}} \tag{2-34}$$

since

$$X \equiv \int_o^\infty r^2 \; \frac{E_s}{E_o} \; dr$$

we have

$$X = L \; \frac{\hat{\bar{L}}_{11}(180)}{4\pi} \int_o^\infty e^{-\frac{2\tau(Z)}{\cos\psi}} \; \beta(Z)\, dr \tag{2-35}$$

Since

$$Z = r\cos\psi \quad \text{and} \quad dZ = dr\cos\psi,$$

$$X = \frac{L \; \hat{\bar{L}}_{11}(180)}{4\pi\cos\psi} \int_o^\infty e^{-\frac{2\tau(Z)}{\cos\psi}} \; \beta(Z)\, dZ \tag{2-36}$$

Since

$$\tau(Z) = \int_o^Z \beta(\xi)\, d\xi \tag{2-37}$$

and

$$\frac{d\tau(Z)}{dZ} = \beta(Z)$$

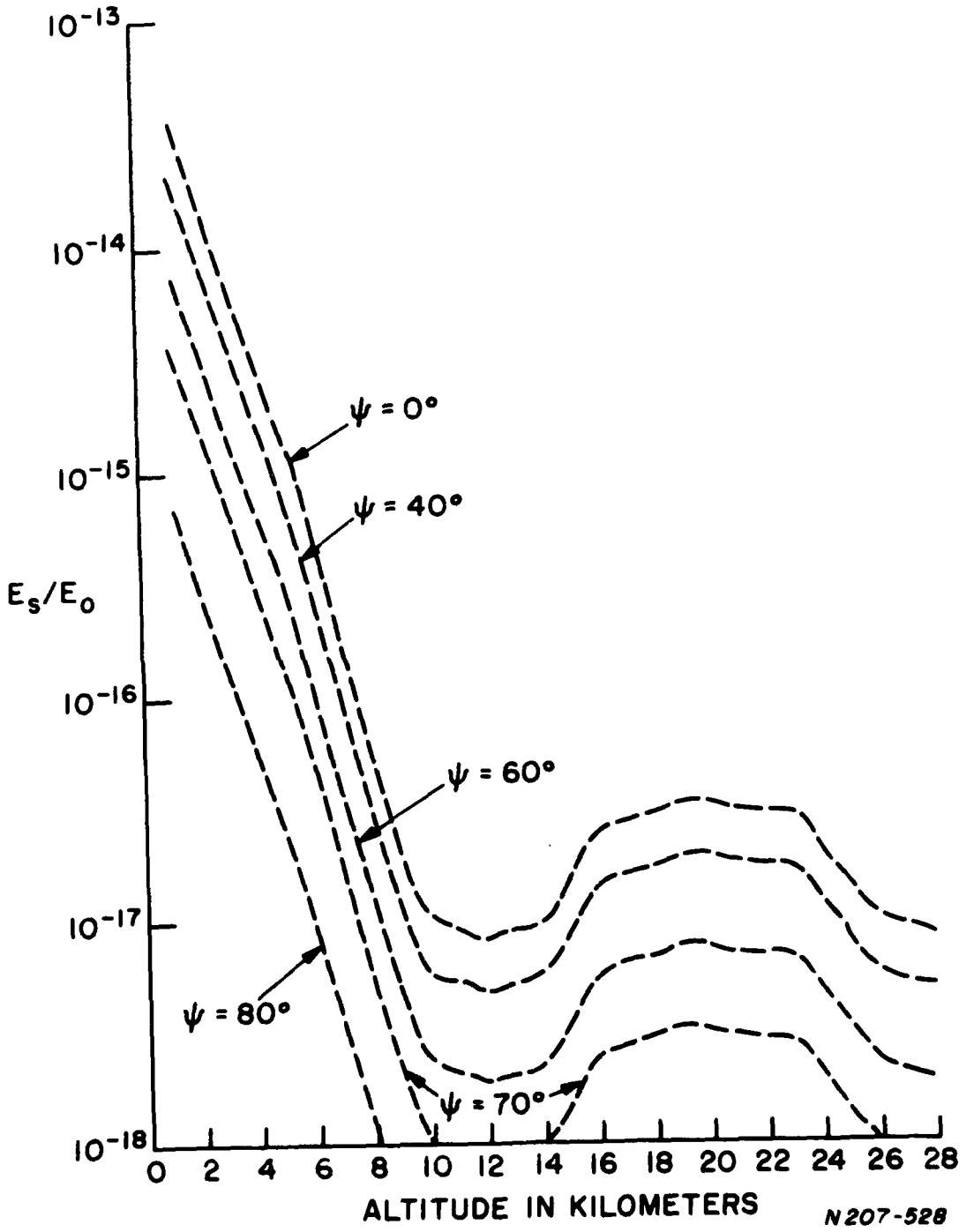

Figure 7. $\frac{E_s}{E_o}$ Per Unit Detector. Area Oriented Normal to the Beam, as a Function of Altitude for Several Zenith Angles. (Elterman Model) λ = 0.7 micron.

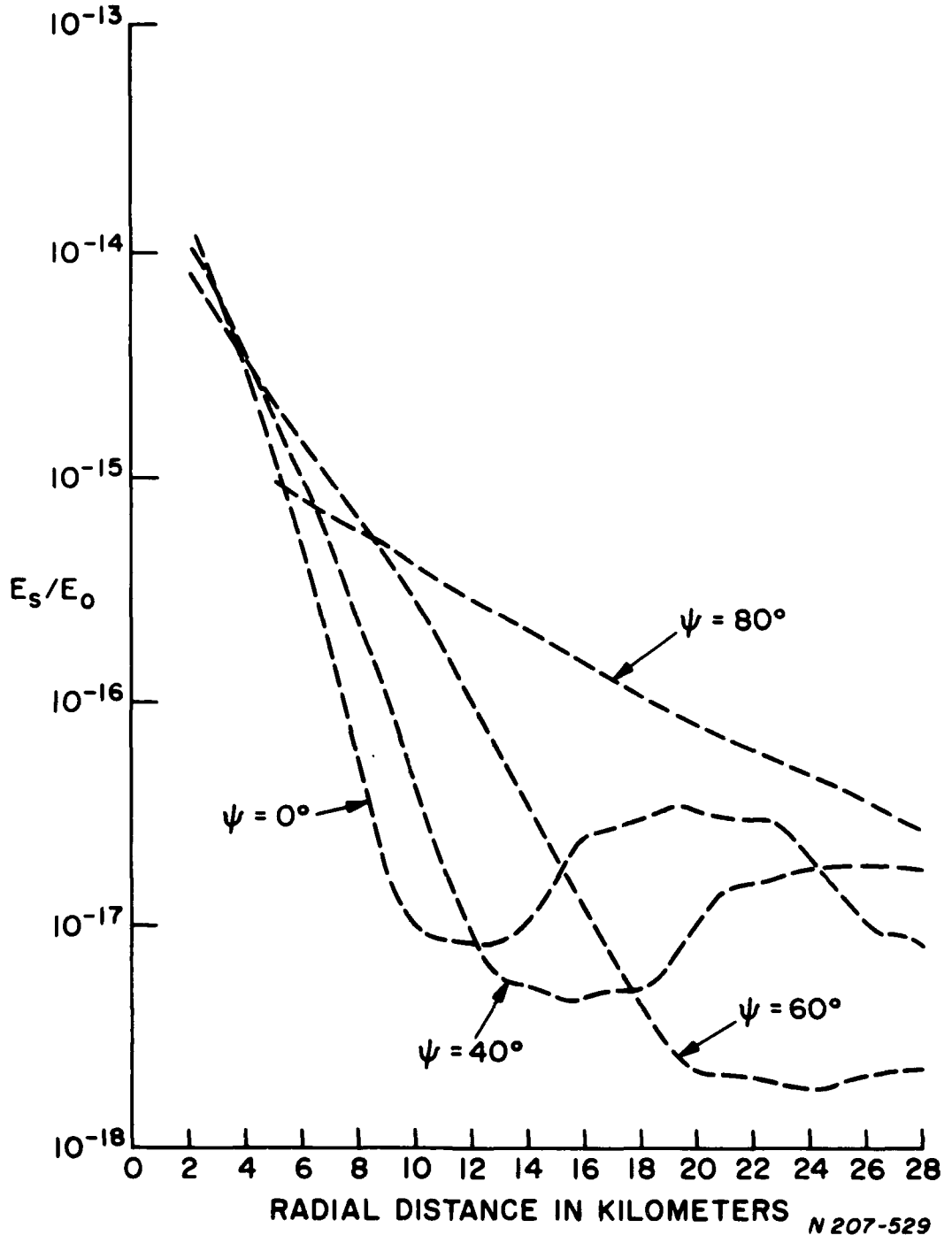

Figure 8. $\frac{E_s}{E_o}$ Per Unit Detector. Area Oriented Normal to the Beam, as a Function of Distance for Several Zenith Angles. (Elterman Model). λ = 0.1 micron.

then

$$X = \frac{L \hat{\bar{L}}_{11}(180)}{4\pi \cos\psi} \int_{\tau(o)}^{\tau(\infty)} e^{-\frac{2\tau}{\cos\psi}} d\tau$$

or since $\tau(o) = 0$,

$$X = \frac{L \hat{\bar{L}}_{11}(180)}{8\pi} \left(1 - e^{-\frac{2\tau(\infty)}{\cos\psi}}\right) \qquad (2\text{-}38)$$

But

$$T^2 = e^{-\frac{2\tau(\infty)}{\cos\psi}}$$

and therefore

$$T^2 = 1 - \frac{8\pi X}{L \hat{\bar{L}}_{11}(180)}$$

or

$$T^2 = 1 - CX \qquad (2\text{-}39)$$

where

$$C = \frac{8\pi}{L \hat{\bar{L}}_{11}(180)}$$

This simple relationship is derived on the basis of the constancy of $\hat{\bar{L}}_{11}(180)$. Changes in the size distribution with altitude would of course alter this. Also note in the coefficient of X, the dependency on L.

In order to account for different pulse lengths which may be encountered in practice, the value of C may be calculated as a function of L, the transmitted pulse length. The graph of Figure 9 shows the results of such a calculation. The value of $\hat{\bar{L}}_{11}(180)$ was assumed constant at 0.259 (from Frazer's calculations) and the value of C is plotted for pulse lengths between zero and 0.60 microsecond.

Further calculations can be made in order to determine the relationship that exists between the atmospheric transmissivity, T, and the backscatter function X. The results of this calculation are shown in the curve of Figure 10.

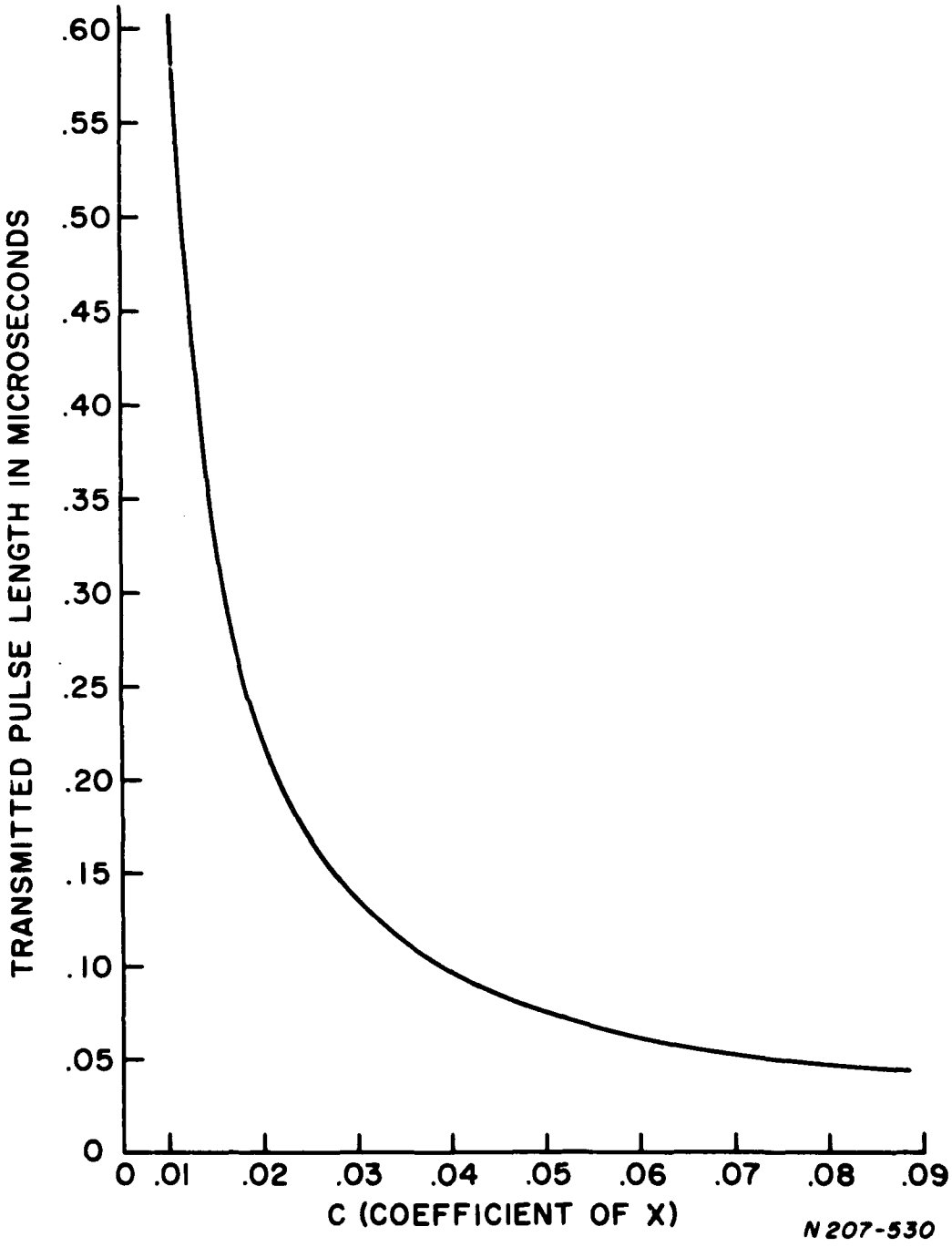

Figure 9. Coefficient of X Plotted as a Function of Pulse Length for $T^2 = 1 - CX$.

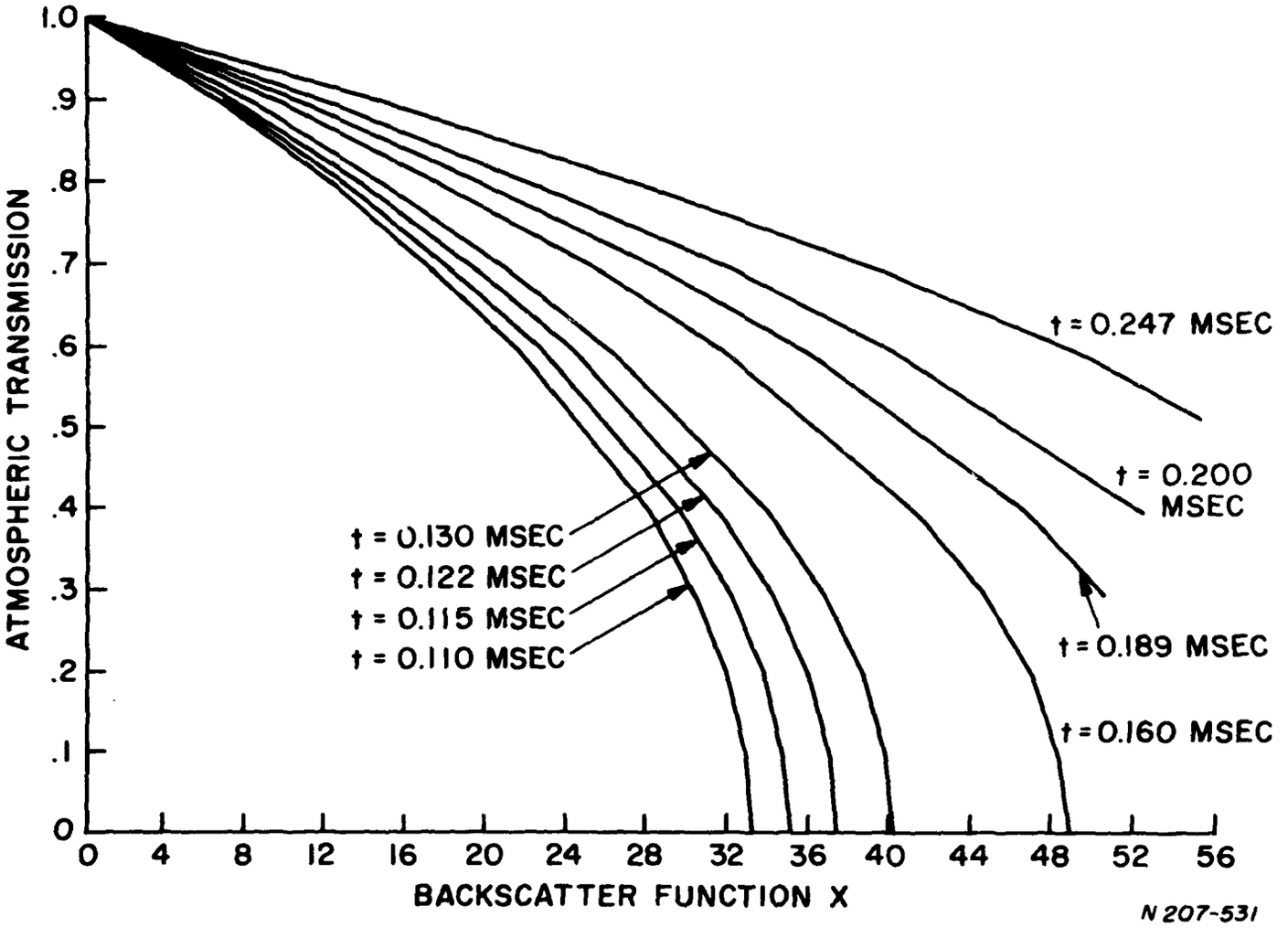

Figure 10. Atmospheric Transmission Plotted as a Function of the Backscatter Function X for Various Transmitted Pulse Lengths.

III. LASER BACKSCATTER MEASUREMENTS

A. Single Color

The theoretical analysis previously discussed, indicated that there exists a relationship between atmospheric transmissivity and the integrated backscatter from a short pulse of monochromatic light, with low transmission corresponding to high integrated backscatter. The program was directed toward exploring this relationship and the results of the work in correlating the data are described in the following paragraphs.

The equipment used to make these measurements consisted of a laser transmitter and receiver and the associated electronics to operate both the transmitter and the receiver.

The transmitter was a ruby laser mounted in a cylindrical cavity with its pump lamp. The pump lamp input energy was normally 1000 joules per shot while the Q-switched ruby laser output was approximately one-half joule. The laser was Q-switched with a spinning roof prism which rotated at about 15,000 rpm. The laser was fitted with a set of beam forming optics which gave an output beam width of about 0.2^{o}.

The receiver was an RCA 7265 photomultiplier tube having an S-20 photocathode and 14 dynode stages. The receiver was fitted with a 100 $\mathring{A}$ bandpass interference filter centered at 6943 $\mathring{A}$. The optics used with the receiver were a sixty-inch f/o.425 mirror with cassegrain secondary. The receiver beam width was 0.33^{o}.

The transmitter and receiver were mounted coaxially with the sixty-inch mirror. This mounting technique was used in order to insure that the transmitted beam was entirely covered by the receiver beam.

The data gathered during this program were taken partly at the Valley Forge Space Technology Center in King of Prussia, Pa., and partly at the Solar Test Facility located at the General Electric Computer Department in Phoenix, Arizona. The change in location was necessary

because the laser was shipped to Phoenix for use on another program. The data obtained was found to be equally valid for both locations when reduced according to the technique described in this paper.

For the data taken at Valley Forge this equipment was mounted on a surplus Army searchlight chassis which provided the pointing capability for the transmitter and receiver. The supporting electronics for this combination were mounted on a second trailer and the trailers were towed into the parking lot at the General Electric Valley Forge Space Technology Center. This equipment is shown in the photograph of Figure 11.

During the data taking period at Phoenix the equipment was mounted on an Antlab model 3544 tracking mount which was housed in a movable building. In operation the building could be rolled back on rails to expose the tracking mount. The photograph of Figure 12 shows the equipment with the building rolled up to cover the tracking mount.

In operation the atmospheric transmissivity is first measured by means of the technique described in Section 2. B. 1 of this report. The laser is then fired along the path toward the star and the backscattered return is recorded by photographing the display on the face of an oscilloscope. A classical "A" scan radar presentation is used which displays received amplitude as a function of range. The time elapsed between the photoelectric measurement of the star intensity and the firing of the laser varied from not less than four seconds to not more than ten seconds. The data collected from each shot are the sky background intensity, the photoelectric intensity of the star, its elevation above the horizon in degrees and two oscillograms. One oscillogram is the "A" scan of the backscattered light while the other shows the output of a transmitter pulse detector. This latter oscillogram is necessary in order to obtain information on the transmitted pulse length, L, and the transmitted energy, E_o. Some samples of the type of data obtained in the oscillograms are shown in Figure 13. Figure 13b shows a typical laser output pulse.

Figure 11. Photograph of the Trailer Mounted Laser Radar.

Figure 12. Photograph of the Laser Radar Mounted on an Antlab Model 3544 Tracking Mount.

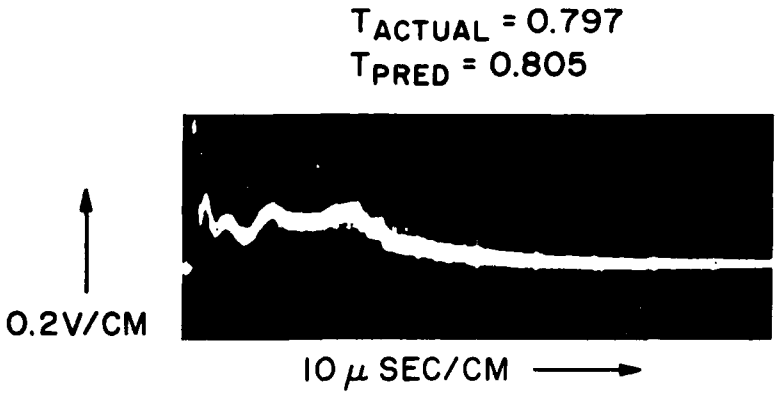

(a) TYPICAL "A" SCAN OF BACKSCATTERED LIGHT FROM CLEAR ATMOSPHERE

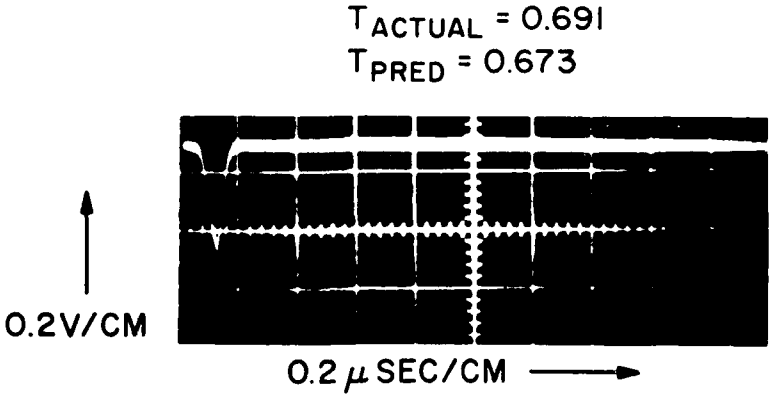

(b) TYPICAL LASER OUTPUT PULSE

Figure 13. Typical Oscillograms Obtained with Laser Atmospheric Probe.

The next set of steps in the data reduction involve the backscatter data and the prediction of the atmospheric transmission. The amplitude of the backscatter return is read from the photograph of the oscilloscope trace with an Analog Oscillogram Reader (Oscar J). The amplitude is read at every change in slope of the return signal and an IBM card is punched for each point read. A computer program has been written which accepts the cards, establishes a data point for each microsecond of time, multiplies the amplitude at each point by the square of the time from the start of the trace, and sums the result of each operation. For each trace of backscatter then a number,

$$f(X) = \sum_t A_t t^2$$

is obtained which is a function of the backscattered light intensity where A_t is the amplitude of the backscattered light at some time t, t^2 is the square of the time to that particular amplitude element (used to compensate for the inverse square behavior with range).

The oscilloscope trace showing the outline of the transmitted pulse is next reduced by determining the pulse height and width and obtaining the area of the pulse by using a traiangle approximation. The area of the transmitted pulse is proportional to the total transmitted energy.

The intended backscatter is now normalized by dividing the integrated backscatter by the area of the transmitted pulse.

$$\overline{F(X)} = \frac{\sum_t A_t t^2}{g(E_o)}$$

where $g(E_o)$ is the measured function of the transmitted pulse energy. The atmospheric transmission is now predicted from the normalized backscatter data by the following process.

We have already suggested that a relationship between the atmospheric transmission, T, and the backscatter from the laser beam exists. The backscatter function is determined by a parameter X which is defined by

$$X = \int_0^\infty \frac{r^2 E_s}{E_o} \, dr, \text{ where}$$

r = radial distance from the source

E_s = backscattered energy (per unit area normal to the transmitted pulse direction).

E_o = transmitted pulse energy.

The laser transmitted pulse detector is calibrated so that by determining the area under the oscillogram of the transmitted pulse, the transmitted energy may be obtained. The receiver is calibrated in terms of receiver energy per unit time. The calibration constants are then applied to the calculated values of $f(X)$ and $g(E_o)$. The predicted atmospheric transmissivity is finally obtained by calculation from equation (2-39).

The final step in the process is to plot the measured transmissivity as a function of the predicted transmissivity obtained from the laser backscatter measurement. This plot is shown in the graph of Figure 14. In Figure 14 the solid line extending from the origin upward to the right is the line of zero error, that is for any point lying on this line there is no error in the transmission measured from the laser backscatter. The two dashed lines indicate the limits of $\pm$ 5% error. The information contained on this plot does indicate that a correlation is remarkably good. It is felt that if the system errors were reduced, both those resulting from inadequacies in the equipment and those introduced by the data reading technique used, that the correlation could be further improved. Additional data both at a higher pulse rate and over a much wider range of atmospheric transmission are desirable in order to improve the correlation.

In order to obtain a comparison between the actual backscatter obtained and that predicted for different types of scatterers the graphs of Figure 15 and 16 were made. The curves of Figures 15 and 16 show the normalized

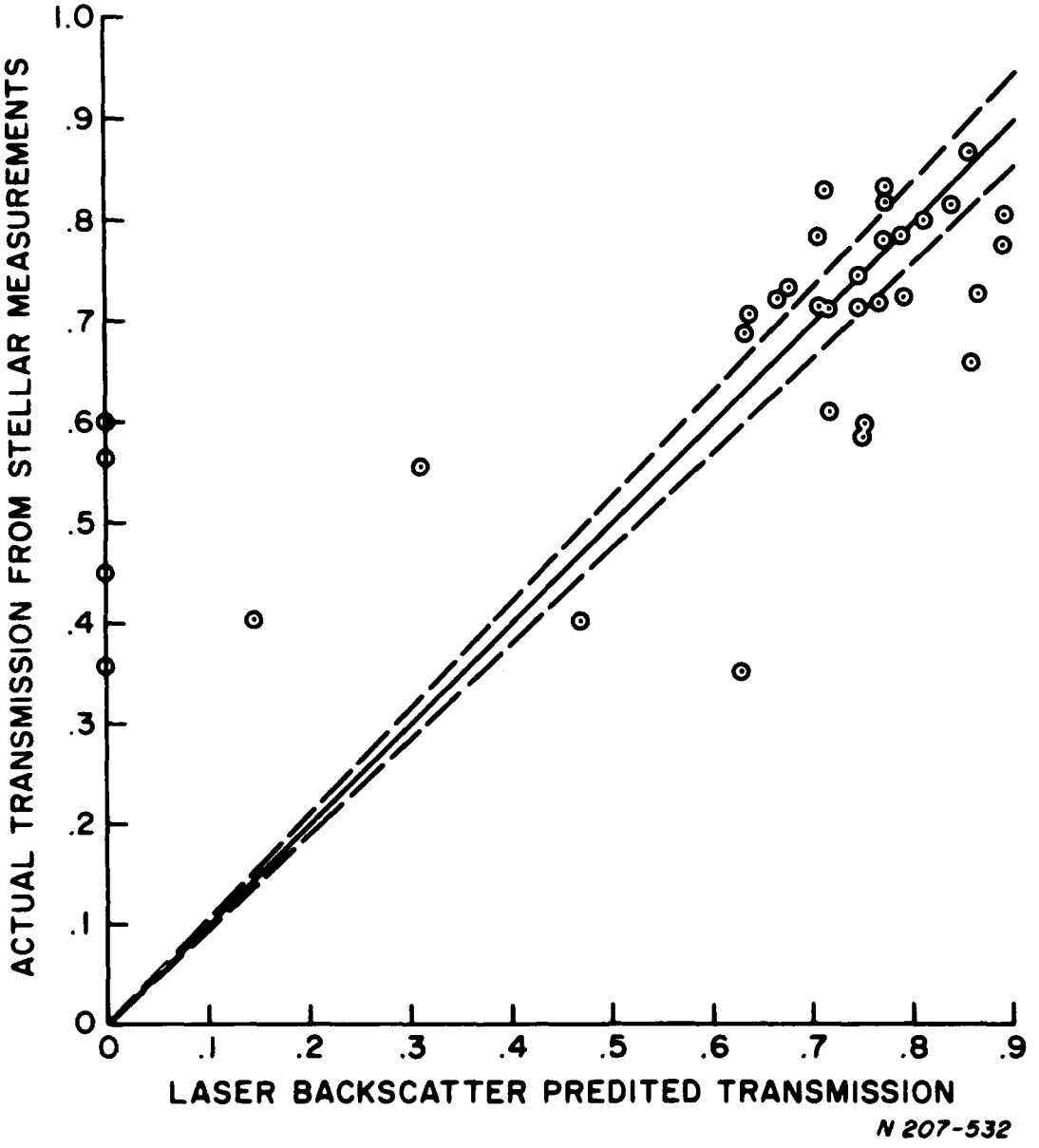

Figure 14. Actual Atmospheric Transmission as a Function of Transmission Predicted by the Laser Backscatter Measurement.

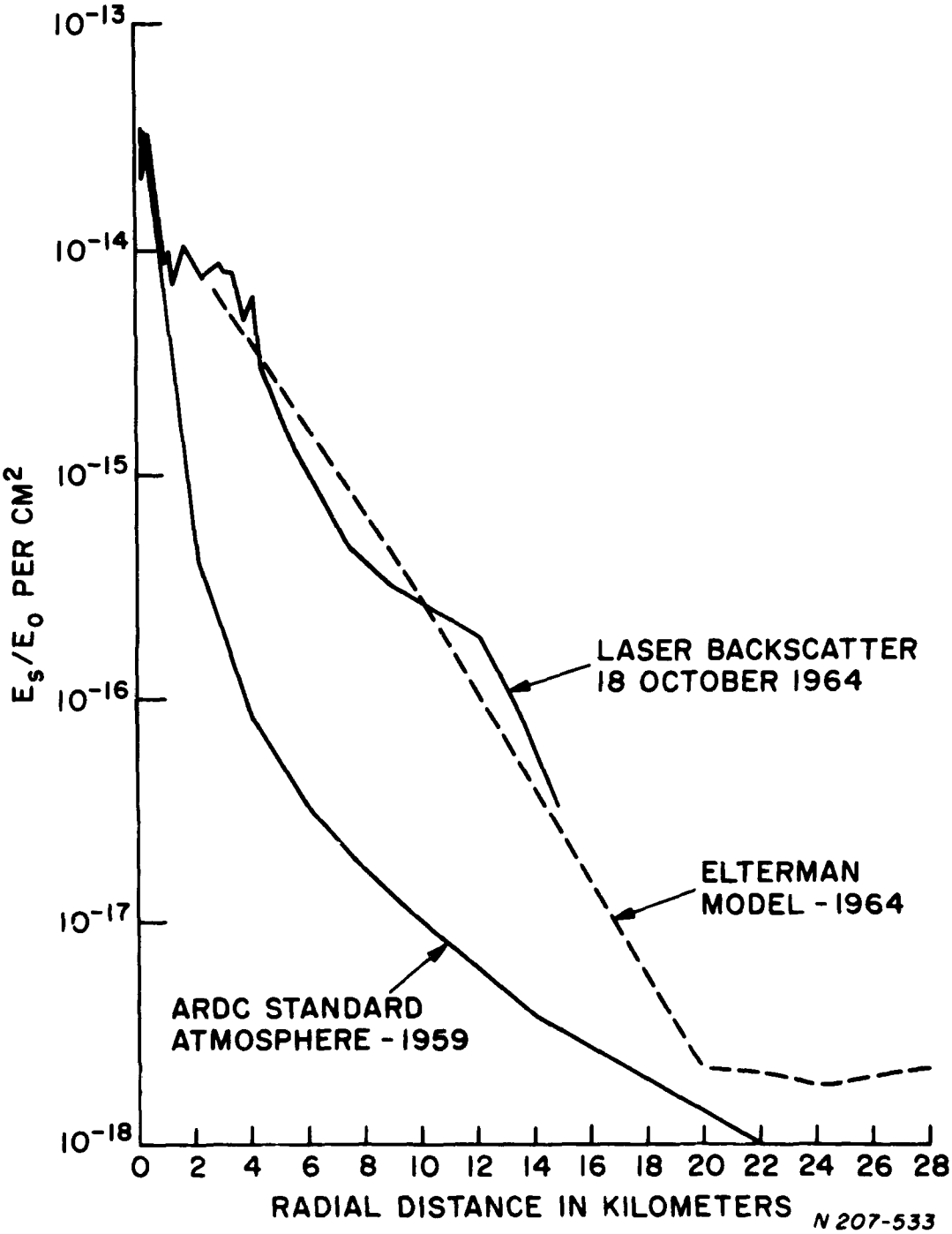

Figure 15. Received Power Per Unit Detector Area Transmitted Power Oriented Normal to the Beam Plotted as a Function of Radial Distance for Zenith Angle of 60°.

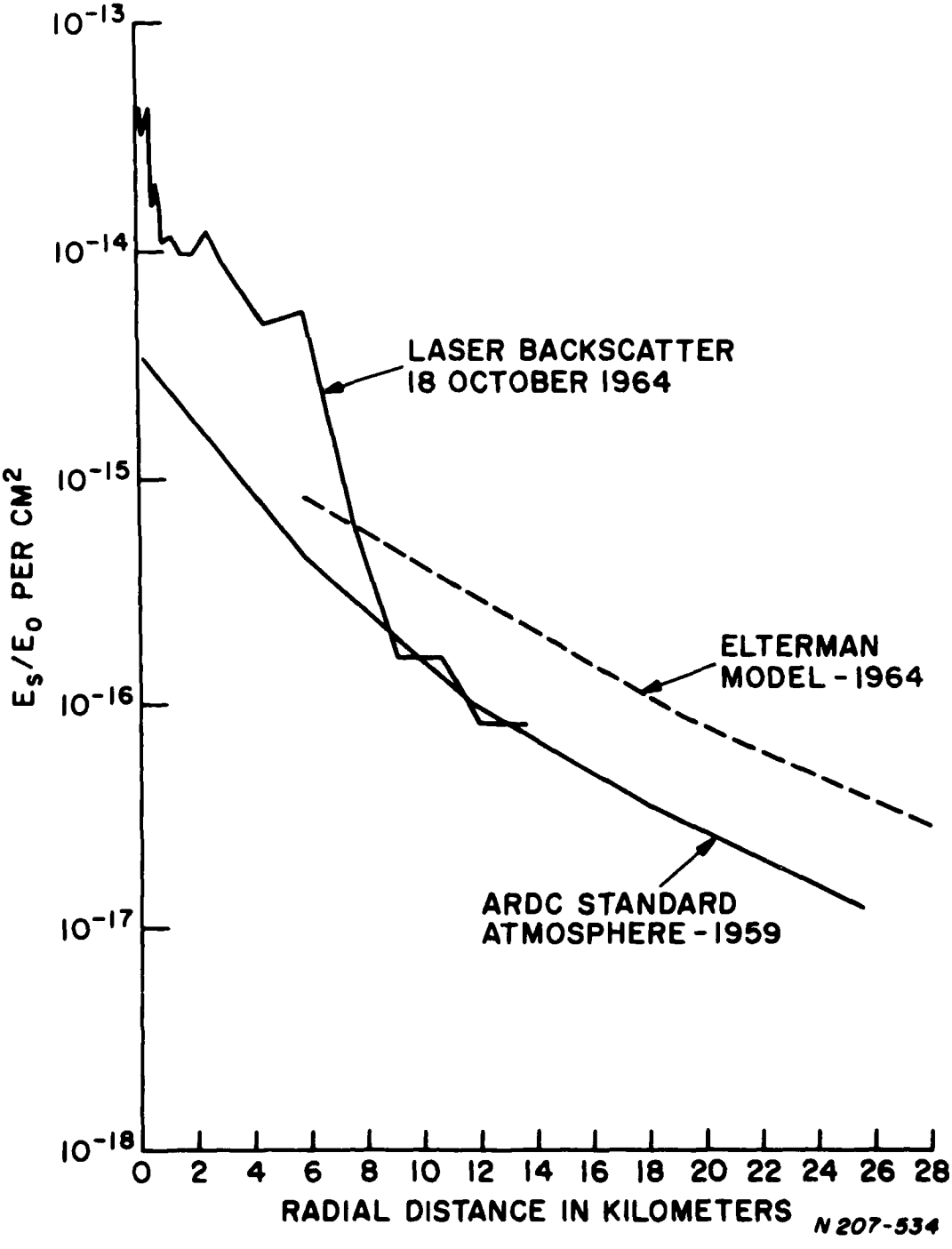

Figure 16. Received Power Per Unit Detector Area Transmitted Power Oriented Normal to the Beam. Plotted as a Function of Radial Distance for Zenith Angle of 80°.

received energy per unit detector area as a function of radial distance in kilometers for three sets of data. The first, the heavy solid line, is for the amount of backscattered energy predicted for Rayleigh scattering. The ARDC Standard Atmosphere for 1959[13] was used to obtain the atmospheric density as a function of altitude. The second curve, the dashed line, is for the amount of backscattered energy predicted from Mie scatterers. The atmospheric model given by Elterman[11] was used to obtain the particle distribution of Mie scatters. The third curve represented by the thin line, is the actual backscattered light energy received. The data shown in Figures 14 and 15 were chosen to illustrate the types of backscatter returns obtained. Figure 14 illustrates a return which corresponds very nearly to the backscattered energy predicted by Elterman's data. The curve of Figure 15, however, shows that in this case the backscattered energy is relatively high for the first five kilometers and then drops to the value predicted for Rayleigh scattering for the remainder of the curve. It is important to note that the predicted values for the backscattered energy from Rayleigh and Mie scatterers is continuous down to zero range and that the curve for Rayleigh scattering is almost exponential (following density variations in the atmosphere). The available data which were used for the predictions, however, was not continuous to zero range since the first given data point was at an altitude of 0.1 kilometer.

Rayleigh scattering has been detected with this equipment to altitudes of 60 kilometers. A laser radar similar to the one used in this program could be used to obtain data on atmospheric density at high altitudes by observing the light backscattered from molecules (Rayleigh scattering) and predicting the density by a technique similar to the one used in this report. It has been calculated that a one-joule laser with a 60-inch receiver could be capable of obtaining good density data at altitudes of up to 100 kilometers.

The primary problem area encountered during this program was the laser itself. With the laser used it was almost impossible to obtain single pulse operation for any extended period of time. Generally the laser would put out two or more giant pulses within a period of about a microsecond. This was caused by the type of Q-switch used and the extreme sensitivity of the ruby rod to changes in the ambient temperature. Early in the program considerable difficulty was encountered with fluorescence from the ruby rod giving false indication of backscattered signal. This was controlled by installing a spatial filter in the colimating telescope used with the laser. Future measurements should be made with a liquid cooled laser which would insusceptible to ambient temperature changes. In addition, a passive Q-switch would be used to improve the single pulse operation of the laser. Quite a number of data points were taken in which two or more giant pulses were obtained from the laser. Efforts to reduce these data to some sensible meaning have so far proved fruitless.

Another problem area encountered both at Valley Forge and at Phoenix, Arisona, was the high sky noise level. This high noise level was caused in both cases by the scattered light from parking lot lights immediately surrounding the transmitter-receiver and by scattered light from the large number of homes, street lights and shopping centers in the area surrounding the test site. The light scattered by the aerosol raises the background level and reduced the signal to noise ratio of the photoelectric measurements. Measurements close to the horizon were particularly difficult to make at Phoenix for this reason and impossible to make at Valley Forge. In both cases we were able to have the nearby parking lot lights turned off which gave some improvement but a large amount of scattered light remained. The only celestial object bright enough to use for these measurements was Jupiter. This was true both at Phoenix and at Valley Forge. The signal to noise ratio on Saturn was too low due to the high noise level. Several stars were tried at Valley Forge; these were Vega, Altair and Arcturus. No useful data were obtained from any of these. At Phoenix these same stars were tried but both the high noise level and scintillation made these data useless.

The reading of the data from the photographs presented the greatest source of possible error in the entire process. In order to keep this error to a minimum the amplitudes were read on an Oscar J oscillogram reader.

A remaining source of error is the determination of the width of the transmitted pulse. The triangle approximation for the area is quite good, but reading the pulse width in exactly the same fashion each time is extremely difficult. It is possible to construct an all electronic data processing equipment which would perform most of these functions automatically. It would be advisable in future work to build some parts of a data processor in order that a greater degree of precision could be obtained in reducing the data.

At the start of the program it was intended that some tropospheric soundings be made during daylight hours. It was found that backscatter data could not be obtained during the daylight hours due to the high noise level. The noise level could be reduced sufficiently low to obtain daylight soundings if a different main receiver mirror of longer focal length were available. The present mirror is sixty-inches in diameter with a 25.5-inch focal length. This gives a f/0.425 optical system. The problem with a short focal length system is that the minimum angle of incidence on the interference filter used in front of the photomultiplier is approximately 10° with an f/0.425 system. These narrow band interference filters have the property that at angles of incidence other than 0° their bandpass is shifted toward the blue. It is therefore necessary with the f/0.425 system to use a 100 Å bandpass filter centered at the ruby laser wavelength. With an f/2 system for example, it would have been possible to use a much narrower bandwidth filter which would reduce the amount of noise taken into the receiver while still allowing the signal light to enter the photomultiplier.

B. Multiple Color

If data could be taken simultaneously at two or more wavelengths then the atmospheric transmission could be obtained over a wide range of wavelengths instead of at a single wavelength. Multiple wavelength measurement would also provide data on the particle size distribution

which would serve to improve the precision of the measurement.

It is fortuitous that laser wavelengths exist at excellent positions throughout the visible and near infra-red spectral areas for this purpose. For example, if one starts with the Neodymium line at 1.06 micron and the ruby line at 6943 Å each may be doubled in a non-linear device such as an ADP crystal[12]. Conversion efficiencies as high as 25% have been reported with 50% being the theoretical maximum. This would give wavelengths of 1.06 micron, 0.6943 micron, 0.5300 micron and 0.3472 micron. The lower energy outputs at the shorter wavelengths is more than offset by the increasing quantum efficiency at the shorter wavelengths in available photomultiplier tubes.

IV. SUMMARY

It has been shown that the application of the single ended telephotometer provides a technique for obtaining error free data on atmospheric transmissivity. The experimental results obtained with a ruby laser used in such an application support the analytical result and indicate that atmospheric transmissivity can be predicted by examining the light backscattered from a pulsed light source. The results of the experimental work are plotted graphically with the predicted result and the two sets of data are in good agreement. A logical extension of this work would be to utilize a four color laser radar operating at 1.06, 0.6943, 0.5300 and 0.3472 micron in order to determine particle size distribution of the atmospheric aerosols at various times and locations. The result of this work would be a series of mean continental aerosols which could be selected for use based upon observable conditions.

Sufficient data were also collected which indicate that atmospheric density to altitudes of at least 100 kilometers can be measured with the ruby laser radar.

ACKNOWLEDGMENTS

The writers wish to thank Dr. J. M. Levin who abstracted and explained portions of Van DeHulst book, The Scattering of Light by Small Particles and Dr. S. R. Hurst who spent many hours in the early stages of the preparation of this report proofreading and suggesting ways of improving the quality of the text.

BIBLIOGRAPHY

1. Admiralty Research Laboratory, "Portable Star Photometer for Measurement of Atmospheric Transmission." Report A. R. L. /N. 3/ E. 600 (Seen in Abstract).

2. Allen, C. W., Atmospheric Refraction and Air Mass, Page 115, "Astrophysical Quantities", Athlone Press, London (1955).

3. W. E. K. Middleton, Vision Through the Atmosphere, page 175 ff, University of Toronto Press 1958.

4. Collier, L. J. "Visual Telephotometry" Transactions of the Illuminating Engineering Society (London) Vol. 3 pp 141-154 (1938).

5. Foitzik, L. "Uber die Lechtdurchlassigkeit der stark getrubten Atmosphare im sichtbaren Spektralbereich." Wiss. Abh. Reichsamt f. Wetterdienst, Berlin 4 No. 5 (1938) (Seen in abstract).

6. Middleton, W. E. K. "The Effect of the Angular Aperture of a Telephotometer on the Telephotometry of collimated and uncollimated beams." Journal of the Optical Society of America, Vol 39 pp 576-581 (1949).

7. Allard, E. "Memoire sur l'intensite et la portee des phares." Paris Punod, p 70 (1876) (Original not seen but the section in question was reprinted in Reference (3).

8. Personal communication from Dr. J. M. Levin, General Electric Co. Space Sciences Laboratory. This discussion and notation follows closely that of Van de Hulst H. G. The Scattering of Light by Small Particles.

9. Fraser, R. S., "Scattering Properties of Atmospheric Aerosols", Scientific Report No. 2, Contract No. AF19(604) 2429 UCLA, Oct. 1959.

10. Gray, E. L., (July 22, 1964) Backscatter and Transmission of a Laser Pulse, General Electric Internal document.

11. Elterman, L. Environmental Research Paper No. 46. "Atmospheric Attenuation Model 1964, in the Ultraviolet, Visible and Infrared Regions for Altitudes to 50 KM," AFCRL-64-740. (September 1965).

12. Minck, R. W., "Nonlinear Optical Phenomena" a paper presented at the Northeast Electronics Research and Engineering Meeting, Boston, Mass. November 4-6, 1963 (Paper No. TAM 8.4).

13. The ARDC Model Atmosphere (1959), Air Force Cambridge Research Center.

14. Allen, C. W., Astrophysical Quantities pp 114-115, The Athlone Press 1955.